HHS Public Access
Author manuscript
J Biomech. Author manuscript; available in PMC 2017 August 16.

Published in final edited form as:
J Biomech. 2016 August 16; 49(12): 2548–2559. doi:10.1016/j.jbiomech.2016.03.023.

Microstructure-Based Biomechanics of Coronary Arteries in Health and Disease

Huan Chen[1] and **Ghassan S. Kassab**[1]
[1]California Medical Innovations Institute, Inc., San Diego, CA92121

Ghassan S. Kassab: gkassab@calmi2.org

Abstract

Coronary atherosclerosis is the major cause of mortality and disability in developed nations. A deeper understanding of mechanical properties of coronary arteries and hence their mechanical response to stress is significant for clinical prevention and treatment. Microstructure-based models of blood vessels can provide predictions of arterial mechanical response at the macro- and micro-mechanical level for each constituent structure. Such models must be based on quantitative data of structural parameters (constituent content, orientation angle and dimension) and mechanical properties of individual adventitia and media layers of normal arteries as well as change of structural and mechanical properties of atherosclerotic arteries. The microstructural constitutive models of healthy coronary arteries consist of three major mechanical components: collagen, elastin, and smooth muscle cells, while the models of atherosclerotic arteries should account for additional constituents including intima, fibrous plaque, lipid, calcification, etc. This review surveys the literature on morphology, mechanical properties, and microstructural constitutive models of normal and atherosclerotic coronary arteries. It also provides an overview of current gaps in knowledge that must be filed in order to advance this important area of research for understanding initiation, progression and clinical treatment of vascular disease. Patient-specific structural models are highlighted to provide diagnosis, virtual planning of therapy and prognosis when realistic patient-specific geometries and material properties of diseased vessels can be acquired by advanced imaging techniques.

Keywords

Constitutive model; atherosclerosis; elastin; collagen; smooth muscle cells

Correspondence to: Ghassan S. Kassab, gkassab@calmi2.org.

CONFLICTS OF INTEREST STATEMENT
The authors certify that they have NO affiliations with or involvement in any organization or entity with any financial interest, or non-financial interest in the subject matter or materials discussed in this manuscript.

1. INTRODUCTION

Coronary artery disease (CAD) is the major cause of mortality and morbidity in Western countries (Roger et al., 2012). CAD is caused by plaque buildup in the coronary artery wall that narrows the vessel lumen over time and blocks blood flow to the heart muscle, which may cause myocardial infarction that may progress to heart failure (Klein and Gheorghiade, 2004). The mechanical properties of coronary arteries are fundamental to the understanding of atherogenesis that strongly affect the stresses and strains in the cells and fibers of the arteries. Knowledge of mechanical response of arteries can also greatly advance the preoperative assessment of therapies; e.g., stent implantation using a patient-specific computational analysis (Antoniadis et al., 2015). Accurate model predictions of the mechanical properties of arterial wall under physiological and pathological loading are necessary for clarifying the initiation, progression and clinical treatment of vascular disease.

Microstructure-based constitutive models for blood vessel are motivated by the fact that the overall vascular mechanical properties stem from microstructural components including elastin and collagen fibers, smooth muscle cells (SMCs), and the ground substance. These models can accurately predict the macro- and micro-level mechanical behavior of arteries to provide a deeper understanding of the individual role of each constituent. The goal of this review is to provide an overview of coronary artery microstructure including elastin, collagen and SMCs under various loadings. The microstructure is then integrated into mathematical models of mechanical properties to predict vessel responses when mechanical loading is perturbed. The needs for future research directions on micro-mechanical modeling of blood vessels in health and disease are highlighted.

2. MORPHOLOGY AND MECHANICS OF CORONARY ARTERIES

The morphology of artery wall has been investigated extensively for several decades (Rhodin, 1980; Bunce, 1974; Smith et al., 1981; Hass, 1942; Finlay et al., 1995; Zoumi et al., 2004; Chen et al., 2011a, 2013b, 2013a). The arterial wall is composed of three distinct layers including intima, media and adventitia, respectively (Rhodin, 1962). For many types of arteries such as aorta, carotid, iliac (elastic arteries) and coronary (muscular artery), the layers consist of common components such as collagen, elastin and SMC, albeit the ultrastructure of each artery is unique with specific content and arrangements of constituents in individual layers (Rhodin, 1980; Smith et al., 1981; Haas et al., 1991; Finlay et al., 1995). The microstructure of coronary arteries is the major focus of this review as described below.

2.1 Structure of Normal Coronary Arteries

The adventitia (outermost layer of an artery) typically consists of dense collagen fibers, elastin fibers, some fibroblasts and hydrophilic macromolecules (including glycosaminoglycans, proteoglycans and glycoproteins), and serves to protect the vessel wall from over-stretch as well as to mechanically couple to the surrounding tissues (Clark and Glagov, 1985; Zoumi et al., 2004). Classical histological studies showed that fibers in adventitia rendered a preferred orientation in non-coronary arteries (Rhodin, 1980; Smith et al., 1981; Haas et al., 1991; Finlay et al., 1995). Zoumi et al. (Zoumi et al., 2004) combined two-photon-excited fluorescence (TPEF) microscopy and second harmonic generation

(SHG) microscopy to visualize elastin and collagen fibers simultaneously in porcine coronary arteries, and found that the adventitia is rich in collagen bundles and a few elastin fibers oriented in the direction along the vessel axis.

Recently, Chen et al. (2013b, 2011a) examined more detailed longitudinal-circumferential sections (Fig. 1) of coronary arteries and revealed that elastin and collagen fibers form concentric densely packed fiber sheets in inner adventitia (Fig. 1b), and collagen fibers largely orient towards the axial direction of the artery with a peak at 110° (0° denotes circumferential direction and 90° denotes axial direction) (Fig. 1c). Elastin was parallel with collagen fiber but with secondary direction forming a netlike structure in a sublayer (Fig. 1d). Collagen fibers gradually become thicker and distributed randomly toward the exterior adventitia whereas elastin fibers were largely absent. The ratio of collagen content (33.5%) to elastin content (22.1%) in adventitia of the left anterior descending (LAD) coronary arteries was reported as 1.5 (Chen et al., 2011a), which was higher than the ratio of 1.1 for the right coronary arteries, RCA (Garcia and Kassab, 2009). The difference was likely due to different branches (LAD vs. RCA) and size of animal (body weight of 80 kg vs. 43 kg). The morphometry of elastin and collagen fibers are shown in Fig. 2a–c and quantitative data of microstructure of coronary arteries are summarized in Table 1.

The media layer of an artery serves as the most important mechanical layer at physiological conditions (i.e., under normal hemodynamic loadings) (Rhodin, 1980). The media is made up of concentric SMC layers, elastic lamellae (EL), collagen fibril bundles and elastic fibrils. For most arteries, EL are thick continuous sheets of elastin with periodic pores, and SMCs fill within inter-lamellae (IL) space and connect to dense and intricately organized IL elastin fibers, while collagen bundles intersperse between EL and enveloped SMCs (Clark and Glagov, 1985; O’Connell et al., 2008). Coronary media EL is composed of narrower and more widely spaced elastin fibers (Clark and Glagov, 1985) and thus presents a thin and porous structure compared to aorta (e.g., compare Fig. 1 and Fig. 2 of Zoumi et al., 2004). Moreover, the IL space becomes wider and may contain more than one layer of SMCs (Clark and Glagov, 1985; Zoumi et al., 2004). A later study of Boulesteix et al. (Boulesteix et al., 2006) found that murine coronary arteries do not contain many elastin laminae as found in aorta and carotid arteries. It was reported that the volume density of SMC was 74% while that of extracellular matrix (i.e., collagen and elastin fibers, ECM) was 17% for adult murine coronary media (Cebova and Kristek, 2011). The ratio of collagen to elastin content was 3.7 in media layer of porcine RCA (Garcia and Kassab, 2009) which was slightly larger than that of intact coronary arteries (e.g., ratio of intact canine coronary arteries was reported as 3.1 by Fischer and Llaurado, 1966) likely due to the lower ratio of collagen to elastin in adventitia.

The arrangement and orientation of SMCs show variations depending on types of arteries and species (Wolinsky and Glagov, 1967; Osborne-Pellegrin, 1978; Hansen et al., 1980; Rhodin, 1980; Clark and Glagov, 1985; O’Connell et al., 2008; Fujiwara and Uehara, 1992). For bovine coronary arteries, previous studies found SMCs have a longitudinal arrangement in inner and outer layers of media, whereas the cells in middle layers are arranged along the circumferential direction of the vessel (Fischer, 1951; Rhodin, 1980). Quantitative measurements confirmed that SMCs aligned off circumferential direction of porcine coronary media with symmetrical polar angles 18.7°±10.9° (Chen et al., 2013a) as shown in Fig. 2 d. The dimensions and spatial aspect ratio of cells were also determined (Fig. 2e and f). An additional study of 3D reconstruction of SMCs showed that radial tilt angle of cells is about 8 ° (Luo et al., 2015), in line with previous two-dimensional observation. The angle is much smaller than the tilt angle, however, of other tissues (Fujiwara and Uehara, 1992; O'Connell et al., 2008). The quantitative orientation angles of collagen and elastin fibers of coronary media are lacking, however, due the complex 3D architecture of fiber networks. Arrangement of medial collagen is somewhat controversial in the literature. Collagen was commonly described as a meshwork of helically woven fibers layered around the vessel circumference in several previous studies (Rhodin, 1980; Clark and Glagov, 1985; Shadwick, 1999; Walker-Caprioglio et al., 1991) while a later study of 3D microstructure of aortic media suggested that collagen fiber bundles were parallel within each layer and preferentially oriented in the circumferential direction as SMCs (O'Connell et al., 2008). Nevertheless, these studies concur that collagen largely orients towards circumferential direction of vessels, while elastin presents a complex 3D arrangement, including layered EL, randomly distributed IL fibrils and radial thick fibers (O'Connell et al., 2008).

The intima (innermost layer of an artery) consists of endothelial cells, a few collagen bundles and basal lamina (Rhodin, 1980; Zoumi et al., 2004). Rhodin found that the subendothelial area contains bundles of longitudinally arranged SMCs, which is consistent with the longitudinal arrangement of inner media SMCs. The intima is very thin and does not contribute to the mechanical properties of the vessel wall in normal animals (Zoumi et al., 2004; Wagenseil and Mecham, 2009). Velican et al. (Velican and Velican, 1985), however, pointed out that a healthy human coronary artery has a thick intimal layer which develops rapidly in early years and continues to grow throughout life. Holzapfel et al. (Holzapfel et al., 2005a) reported the ratio of thickness of adventitia, media, intima and the total wall of non-atherosclerotic aged human coronary arteries as 0.4±0.03, 0.36±0.03 and 0.27±0.02, respectively.

2.2 Mechanical properties of Normal coronary arteries

In arteries, elastin fibrils have relatively lower stiffness and larger deformability, which helps to support blood vessels at low pressure, whereas collagen fibers are undulated and do not withstand loads. At high pressure, collagen fibers become straightened and engaged to carry most of the load (Clark and Glagov, 1985; Glagov et al., 1992; Zoumi et al., 2004). Engaged collagen fibers are much stiffer than elastin fiber, leading to a rapid increase in strain-stress curve of blood vessel. The modulus of elasticity of collagen is approximately 400 times greater than that of elastin (Burton, 1954). SMCs, when contracted, achieve active response to physiological loads by altering circumferential as well as longitudinal mechanical properties of blood vessels (Dobrin, 1984; Chen et al., 2013a; Huo et al., 2012, 2013). The contribution of passive SMCs, however, has been debated in the literature. Previous studies (Cox, 1981; Viidik, 1979) have stipulated that SMCs have regulatory function with slight effect on the passive mechanical properties of the arterial wall. The study of Fridez et al (Fridez et al., 2003) contended that SMCs did not affect the mechanical responses of the healthy artery and that differences were only observed under pathological conditions of hypertension. Kochová et al. (Kochová et al., 2012) removed SMCs by Triton® X-100 from carotid arteries and showed that SMCs do not directly influence the mechanical behavior. On the contrary, Silver et al. (Silver et al., 2003) and Sokolis et al (Sokolis et al., 2006) asserted that SMCs share the stress with collagen bundles since SMCs are bound in series with a network of interwoven collagen fibrils. The contributions of passive properties of SMCs have yet been well established and should be further investigated.

The mechanical response of individual coronary layers is a direct result of microstructure (Chen et al., 2011a; Huo et al., 2012, 2013; Chen et al., 2013b, 2013a; Lu et al., 2004; Wang et al., 2006). Largely longitudinal alignment of elastin and collagen fibers of adventitia layer induce a larger axial stress than circumferential stress (Chen et al., 2013b) (Fig. 3a and b), while media layer presents a higher circumferential stress than adventitia and intact wall as shown in Figs. 3c and d (Wang et al., 2006), since the SMCs and fibers orient towards the circumferential direction of coronary arteries (Chen et al., 2013a). These mechanical responses are consistent with an earlier study of Lu et al. where they examined passive elastic moduli of individual layers of coronary arteries (Lu et al., 2004). It was found that in the axial direction, elastic moduli increase in the order of adventitia > intact vessel > media, and in the order of media > intact vessel > adventitia in the circumferential direction. In these swine studies, intima was very thin and thus was considered as part of media layer (i.e., intima-media layer), and the coronary artery were analyzed as a two-layer structure. As noted above, the thickness of human coronary intima is comparable to that of adventitia and media, and hence it was considered as an additional layer (Holzapfel et al., 2005a). Moreover, it was found that the intima is the stiffest layer of the human coronary artery while the media is the softest in the longitudinal direction. Analogous to porcine coronary arteries, human coronary adventitia is stiffer in longitudinal direction and the media is stiffer in circumferential direction.

The active mechanical properties of coronary arteries have also been widely investigated. Many studies showed that blood vessels present an uniaxial vasoconstriction; i.e., contracting only in the circumferential direction with no axial response (Rachev and Hayashi, 1999; Zulliger et al., 2004b; Carlson and Secomb, 2005), assuming completely circumferentially oriented SMCs (Wolinsky and Glagov, 1967; Hansen et al., 1980; Clark and Glagov, 1985; O'Connell et al., 2008). Lu and Kassab (Lu and Kassab, 2007) found considerable axial force changes during carotid and femoral arteries contraction, however, using an isovolumic myograph. The study of Hayman et al (Hayman et al., 2013) also showed that SMC vasoconstriction reduced carotid artery buckling as compared with the relaxed conditions, indicating that SMC contraction may shorten the artery in the axial direction. For coronary arteries, Huo et al. (Huo et al., 2013, 2012) observed that axial force significantly increased and outer diameter decreased during K^+-induced SMC contraction under a biaxial protocol of distention and extension. This suggests a biaxial response of coronary arteries; i.e., SMCs contraction induced vessel stiffer in both circumferential and axial directions. Chen et al. (2013a) later measured SMCs orientation of porcine coronary arteries to incorporate into a microstructural model of active coronary media, and revealed that the biaxial vasoactivity is induced by oblique SMC arrangement as well as multi-axial muscle vasoconstriction.

3 STRUCTURAL EVOLUTIONS AND MECHANICAL CHANGES IN AGED AND DISEASE CORONARY ARTERIES

The structural growth and remodeling (G&R) in normal arteries is generally accompanied by increased collagen fibers, hypertrophic SMCs and fragmentation of internal elastic membrane that leads to enlarged diameter and thicker wall of coronary artery. As aging occurs, SMCs progressively migrate from the media and accumulate into the intima which results in intimal hyperplasia (Velican and Velican, 1985). It was reported that coronary intimal thickening is gender- and branch anatomy-dependent (Velican and Velican, 1985, 1981a, 1981b). The vessel size, arterial bed and species also affect intimal thickening (Stout et al., 1983). In intimal thickening, there is an increase in the number of subendothelial cells, which are mainly mononuclear and SMCs (Folkow and Svanborg, 1993; Lakatta, 1993; Wei, 1992) inducing media thickening along with SMCs hypertrophy (Virmani et al., 1991).

Many studies have shown an increase in the content of collagen in large arteries with increased age (Lakatta, 2000; Schlatmann and Becker, 1977; Tsamis et al., 2013), but this change was found to occur nonlinearly (Myers and Lang, 1946). The structure of collagen fibers was also changed with advanced age, showing an increase in irregularly arranged fibers in the media of lager arteries (Toda et al., 1980). For elastin fibers, it was found that mature elastin has a very long life, of which the half-life is about 40 years (Arribas et al., 2006), in line with many observations that elastin content remained unchanged with age (Faber and MOller-Hou, 1952; Hass, 1942; Briones et al., 2010; Tsamis et al., 2013). Therefore, the decrease in elastin concentration (Hass, 1942) is due to increase of other components, such as collagen fibers. Some studies suggested that glycoprotein eventually disappear from elastin fibrils and cause elastin fragmentation and a reduction of its content with aging (Toda et al., 1980; Robert, 1996; Greenwald, 2007).

Although much efforts have been made to quantify structural change of aorta with age (Tsamis et al., 2013), quantitative data of coronary arteries is limited (Cebova and Kristek, 2011; Ozolanta et al., 1998). Ozolanta examined structural and mechanical properties of 205 human coronary arteries (Ozolanta et al., 1998). The samples were divided into six age groups form 1 year to 80 years. The results showed that with the increase of age, the mean thickness of vessel wall and the outer diameter gradually increase. Both collagen and elastin contents increase in aged coronary. The deformability of vessels declines, while the walls become stiffer with an elevated tangential elastic modulus (related quantitative data is listed in Table 2). A study of septal branch of the left descending coronary artery of control Wistar rat showed that inner dimeter significantly increases compared to wall thickness (57% vs. 14%) from 3 weeks to 52 weeks, while the contents of SMCs and ECM increase 9% and 19% in media, respectively (Cebova and Kristek, 2011). The study showed that aged-induced structural change is highly associated with specimens, species and longitudinal positions. Additionally, Valenta et al. investigated aging effects on residual strain, constitutive relation and stiffness parameter of human coronary arteries (Valenta et al., 2002), based on previous experimental studies (Valenta et al., 1999; Ozolanta et al., 1998). A correlation between opening angle and age was given (as shown in Fig. 4a). Age-related stress-strain relation of arterial wall in circumferential direction has also been determined

(Fig. 4b) to confirm that arterial wall hardening increases rapidly above the age of 30. Stiffness parameter gradually increases with age (this increase is significant above the age of 60), and tends to decrease when the opening angle θ increases (Valenta et al., 2002).

Although G&R of vascular structure is a physiological process that accompanies normal growth, exercise training, pregnancy, aging, etc., the borderline between physiology and pathophysiology, in part, depends on the degree of hemodynamic alterations that affects vascular mechanics (Osborne-Pellegrin et al., 2010; Lacolley et al., 2012; Rafieian-Kopaei et al., 2014; Schwartz et al., 1991). Intimal hyperplasia, the precursor lesion for atherosclerosis, is thought to be stimulated by injury, inflammation, and perturbed hemodynamics that affect endothelial shear stress and intramural wall stress. A study of vein grafting hyperplasia clearly demonstrated a relationship between increased mean wall stress and intimal hyperplasia (Zwolak et al., 1987). Choy et al. showed venous hypertension induced by ligation can cause intimal hyperplasia in superficial veins that were not tethered by the myocardium but only wall thickening in intra-myocardial veins due to differences in wall stress in the two local environments of the same heart (Choy et al., 2006). Choy and Kassab showed differences in coronary wall thickness-to-radius ratio in the left ventricle but not the right ventricle due to local adaptation of stress distribution (Choy and Kassab, 2009). Stent-induced abnormal wall shear and intramural wall stresses have also been shown to contribute to intimal hyperplasia (Chen et al., 2011). The relation between wall stress and atherosclerosis has been investigated in coronary (Zhang et al., 2004) and vertebral arteries (Thubrikar and Robicsek, 1995).

The G&R of blood vessels may be mainly mediated by ECM protein secretion and cell proliferation and migration (Banes et al., 1993; Leung et al., 1976; Lu et al., 2011; Moiseeva, 2001; Niland and Eble, 2012). SMCs are embedded in the ECM and surrounded by an incomplete basement membrane (Dingemans et al., 2000). The ECM interacts with cells to regulate diverse functions, including proliferation, migration and differentiation by integrin receptors, which are the principle receptors for the ECM and serve as a transmembrane link between the ECM and the cellular actin cytoskeleton (Niland and Eble, 2012). The principle function of SMCs is to maintain vascular tone and resistance. Adhesion of contractile SMCs to the ECM is fortified in order to withstand the imposed tension due to hemodynamic forces. Perturbation of stress or stretch on vessel walls activates various heparanases and a cascade of proteases that influence the adhesion of ECM to SMC surface, providing the trigger for phenotypic changes (Ward et al., 2000). For instance, during atherosclerotic plaque development, SMCs transit from a contractile to a synthetic phenotype and begin to synthesize ECM (including different molecules seen only in small quantities in normal vessels), which influences cell proliferation and migration. The cells also modify the ECM by producing matrix metalloproteinase which release cryptic fragments that can stimulate cellular responses (Adiguzel et al., 2009).

In arterial atherosclerosis, the endothelial and SMCs become dysfunctional and the disease is accompanied by excessive fibrosis of intima, fatty plaque formation, proliferation of SMCs, and migration of group of cells such as monocytes, T cells, and platelets (Rafieian-Kopaei et al., 2014; Stary et al., 1995; Virmani et al., 2000). The initial lesion is usually caused by focal increase in the lipoproteins of the intimal layer of the arteries. The lesion grows into fibrous cap atheroma, classically showing a necrotic core (NC) containing cholesterol esters, free cholesterol, phospholipids, and triglycerides. The fibrous cap consists of smooth muscle cells in a proteoglycan-collagen matrix, with a variable number of macrophages and lymphocytes. As lesions progress, NC surrounded by macrophages become increasingly consolidated or more masses comprising large amounts of extracellular lipid, cholesterol crystals, and necrotic debris. Vulnerable plaque generally refers to a thin fibrous cap atheroma, which is distinguished from the earlier fibrous cap lesion by the loss of smooth muscle cells, extracellular matrix, and inflammatory infiltrate. The NC underlying the thin fibrous cap is usually large and hemorrhage and/or calcification are often present. The lesions can be exacerbated to fibrocalcific plaques or develop calcified nodule, and eventually induce thrombosis or vessel rupture (Virmani et al., 2000). According to lesion evolution, the plaques were classified into six types by the American Heart Association (AHA) criteria and seven types by the modified histologic classification of Virmani et al. (Stary et al., 1995; Virmani et al., 2000).

There have been many efforts to identify the components of atherosclerotic plaques of coronary arteries. Romer et al. quantified plaque composition by near-infrared Raman Spectroscopy and provided the relative weights of cholesterol, calcium salts and delipidized arterial tissue in non-atherosclerotic tissues, non-calcified and calcified plaques (Römer et al., 1998). Moore et al. characterized coronary atherosclerotic morphology by a radiofrequency spectral analysis based on intravascular ultrasound (IVUS) images and accurately identified fibrosis, lipid, microcalcification, heavy calcium in coronary arteries (Moore et al., 1998). A later study of Nasu et al. proposed a color-coded mapping method using IVUS radiofrequency data analysis and showed this technique may play an important role in detecting vulnerable plaque (Nasu et al., 2006). Li et al. recently employed high-resolution multicontrast-weighted magnetic resonance technique to identify the composition of atherosclerotic plaques of human left main coronary artery, and accurately classified plaques according to the AHA criteria (Li et al., 2012). These structural changes are associated with significant alterations in the mechanical properties of the arteries. Karimi et al. examined both healthy and atherosclerotic human coronary arteries by uniaxial tensile test and found that the atherosclerotic arteries bear 44.5% more stress and 34.6% less strain as compared to the normal arteries. The physiological and maximum elastic moduli of atherosclerotic arteries are 2.5 and 2.9 times higher than that of healthy arteries, respectively, as summarized in Table 3 (Karimi et al., 2013).

4 MICROSTRUCTURE-BASED MECHANICAL MODELS OF HEATHLY CORONARY ARTERIES

4.1 Microstructure-based Constitutive Model with a Fluid-like Matrix

The idea of relating the macroscopic mechanical properties of arteries to the arterial microstructures, including elastin and collagen fibers and cells, was first demonstrated by Burton and Yamada (Burton and Yamada, 1951). Roach and Burton (Roach and Burton, 1957) made a quantitative study by differential digestion of elastin or collagen and measured the mechanical properties of the digested artery. Azuma and Hasegawa (Azuma and Hasegawa, 1971) discussed the rheological properties of arteries and veins in terms of the networks of collagen, elastin and SMCs, and revealed that the mechanical properties of the vessels largely stem from microstructure.

The first microstructural models were proposed by Lanir (Lanir, 1983, 1979) and Decraemer et al. (Decraemer et al., 1980). Lanir (Lanir, 1983, 1979) considered the passive fibrous tissue as a composite of elastin and collagen fibers, while SMCs and ground substance were assumed to be a fluid-like matrix. Both elastin and collagen embedded the fluid-like matrix, and the fibers only sustain non-hydrostatic loading such as tension and shear while the contribution of the matrix is a hydrostatic pressure. This simplification implies that the fibers deform identically as the tissue, and the overall strain energy function (SEF) of tissue is therefore the volumetric sum of the individual fibers' SEFs. Each fiber has its own SEF $w_i(e)$, which depends on the uniaxial fiber strain $\boldsymbol{e}$ that is determined by the local strain tensor $\mathbf{E}$ and the reference fiber direction $\mathbf{N}$ as $e = \mathbf{E} : \mathbf{N} \otimes \mathbf{N}$. Fiber orientation is determined by $\mathbf{N} = \cos\theta \cos\varphi\ \boldsymbol{e_R} + \sin\theta \cos\varphi\ \boldsymbol{e_\Theta} + \sin\varphi\ \boldsymbol{e_z}$ with $(\boldsymbol{e_R}, \boldsymbol{e_\Theta}, \boldsymbol{e_z})$ as three principle axes of blood vessel. This model involves the orientation distribution of one type of fiber i by a density function $\mathscr{R}_i(\theta,\varphi)$ with θ, φ are azimuthal and polar angles between the fiber direction and principle axes. The overall SEF is the sum of fibers' SEF in all directions (Hollander et al., 2011):

$$W(E) = \sum_i \Phi_i \iint \mathscr{R}_i(\theta,\phi) w_i(e) \sin\theta\, d\theta\, d\phi \tag{1}$$

where Φ_i. is the volume fraction of type i fibers. The second Piola-Kirchhoff stress of the tissue is derived as:

$$\frac{\partial W}{\partial \mathbf{E}} = \sum_i \Phi_i \iint \mathscr{R}_i(\theta,\phi) \frac{\partial W_i(e)}{\partial e} \mathbf{N} \otimes \mathbf{N} \sin\theta\, d\theta\, d\phi \tag{2}$$

in which $\frac{\partial W_i}{\partial e}$ is the stress-strain relation of type i fibers.

The density function $\mathscr{R}_i(\theta,\varphi)$ of fiber orientation can be determined by experimental measurements. Specific to porcine coronary arteries (Chen et al., 2013a, 2011a), elastin and collagen fibers form layered structure in adventitia and the overall fiber orientation follow a bimodal distribution with two peaks, of which the first lower peak is nearly in the circumferential direction and the second higher peak is nearly in the axial direction. In media, large collagen and elastin fibers may be parallel to SMCs aligning off circumferential direction of blood vessels with symmetrical normal distributions, and IL elastin fibrils can be assumed to be distributed following a three dimensional beta function (Hollander et al., 2011).

The constitutive law of a single elastin is considered to be linear, while that of collagen fibers is assumed to be nonlinear (Annovazzi and Genna, 2010; Hollander et al., 2011; Chen et al., 2011b), based on experimental observations (Gosline et al., 2002; Gentleman et al., 2003; Zoumi et al., 2004; Chen et al., 2011a, 2013b). Both types of fibers are only resistant to tensile load (i.e., $e > 0$), and collagen fibers are recruited to carry out loads only after they become straightened. Lanir et al. (Lokshin and Lanir, 2009; Hollander et al., 2011) considered a linear SEF for elastin by $\partial W_E/\partial e = k_E e$ with $k_E > 0$ as stiffness parameter of elastin fiber. Because of the wavy nature of collagen fibers, the nonlinear constitutive relation $\partial W_C/\partial e = k_C(e - e_0)^N$ was considered to account for the nonlinear elastic behavior, of which $k_C > 0$ and $M_C > 0$ are parameters characterizing the nonlinear stress-strain response of collagen, and $e_0 > 0$ denotes the strain beyond which the collagen can withstand tension, as determined by measurements (Chen et al., 2011a). It should be noted that the values of model parameters are highly associated with species and sizes of tested specimens. The microstructural approach, in principle, can employ any well-defined constitutive model for the fibers. This microstructural model accounts for fiber volume fraction Φ_i, the orientation $\mathcal{R}_i(\theta, \varphi)$ and undulation distributions e_0 and is capable of accurately describing and predicting the mechanical properties of blood vessels. The study of Hollander et al. (Hollander et al., 2011) showed the model provides good predictions of coronary media twist response based on parameters estimated from only biaxial tests of inflation and extension. In addition, good predictive capabilities are demonstrated for the model behavior at high axial stretch ratio based on data of law stretches.

Decraemer et al. (Decraemer et al., 1980) proposed a parallel wavy fibers model for soft biological tissues in uniaxial tension based on similar simplifications. A later study of Wuyts et al. (Wuyts et al., 1995) developed his approach by including a distribution of the initial length of collagen fibers to predict blood vessel mechanical properties. Humphrey and Yin (Humphrey and Yin, 1987) also employed fluid-like matrix assumption in a constitutive models of soft tissues. Although these microstructural models have been well developed 40 years ago, the application have been somewhat limited due to lack of quantitative data of tissue microstructure in literature; and the complex integral expression of SEF made it difficult to implement in finite element (FE) simulations. Recently, the microstructure of many tissues have been visualized and measured due to the development of multiphoton microscopy techniques (O’Connell et al., 2008; Chen et al., 2013b, 2013a). Based on quantitative microstructural data, Chen et al extended the model to account for active SMCs contraction and accurately predicted biaxial vasoactivity of coronary arterial media (Chen et al., 2013a). They also developed a layer-specific microstructural model for coronary adventitia to determined material parameters of individual elastin and collagen fibers (Chen et al., 2015). Compared with phenomenological models, these layer-specific models are based on realistic microstructure and the material parameters of individual fibers have physical meaning. The models can accurately predict the mechanical microenvironment of vessel wall and hence elucidate the underlying mechanisms of vessel behavior.

4.2 Microstructure-based Constitutive Model with a Solid-like Matrix

Some micromechanical models assume the tissue as a collagen fiber reinforced composite, whose matrix is a solid-like material that can take up load. This assumption is motivated by the fact that the elastin, which is part of the matrix, becomes straightened and begins to take the load in the early deformation of the tissue. The experimental study of Gundiah et al. (Gundiah et al., 2007) suggested that the elastin is described with a neo-Hookean constitutive model, and later observations of Chen et al. (2013b) confirmed the relatively isotropic arrangement of elastin fibers. Based on this assumption, Holzapfel et al. (Holzapfel et al., 2000) modeled the arterial wall as a two-layer fiber-reinforced composite of which elastin fibers, cells and ground substance are considered as a non-collagenous matrix. The matrix contributes to the isotropic mechanical responses of the blood vessel, while the anisotropic part originates from the deformation of two classes of collagen fibers symmetrically disposed with respect to the axis of the vessel. The SEF of an individual layer of blood vessel is given as:

$$W(E)=\frac{c}{2}(I_1-3)+\frac{k_1}{2k_2}\sum_{i=4,6}\left\{\exp\left[k_2(I_i-2)^2\right]-1\right\} \quad (3)$$

where $c > 0$ is stress-like material parameter of the non-collagenous matrix, and $k_1 > 0$ is stress-like material parmaeters and $k_2 > 0$ a dimensionless parameters for collagen fibers. I_1 is the first invariant of the Cauchy-Green deformation tensor **C**; I_i is an invariant of the Cauchy-Green tensor **C** with respect to the vector v_i of a fiber orientation by $I_i = \mathrm{v}_i \cdot \boldsymbol{C} \cdot \mathrm{v}_i$.

This model has been applied and developed for various tissues (Holzapfel et al., 2005a; Kroon and Holzapfel, 2008; Wan et al., 2012; Avril et al., 2013) and numerical simulations (Gasser et al., 2002, 2006) because of the straightforward mathematical form of SEF. Kroon and Holzapfel (Kroon and Holzapfel, 2008) incorporated the model into multi-layered structures with the mean fiber alignments that distinguished one layer from another. Li and Robertson (Li and Robertson, 2009) extended this model to account for either a finite number of fiber orientations or a fiber distribution function. Mechanical predictions of the model are more accurate than those of phenomenological models as they account for heterogeneity of material properties and geometrical features of vessel components. Since the actual fiber geometrical distributions are not considered, however, the model may not accurately predict stress level of individual fibers and cells and the corresponding material parameters are not physically meaningful.

There have been many other micromechanical models based on solid-like matrix simplification. Zulliger et al. (Zulliger et al., 2004a) employed different SEF of the matrix and collagen fibers to account for the distribution of the waviness of collagen fibers, and this model was developed to predict mechanical responses of aging arteries (Zulliger and Stergiopulos, 2007). Grytz and Meschke (Grytz and Meschke, 2009) approximated the collagen fibril crimp by a three-dimensional cylindrical helix to represent the constitutive behavior of the hierarchical organized substructure of biological tissues. Chen and colleagues (Chen et al., 2011b) assumed non-affine deformation in tissue and developed a finite-strain homogenization approach based on the second-order estimate theory to predict the macroscopic stress-strain relation and microstructural deformation of vascular tissue. Martufi et al. (Martufi and Gasser, 2011) and Sáez et al. (Sáez et al., 2014) developed structural constitutive models of blood vessels, of which collagen fibers are assembled by proteoglycan cross-linked collagen fibrils and reinforce an isotropic matrix material, albeit some experimental observations suggested that proteoglycan plays a negligible role in the elastic behavior of vascular tissues (Viidik et al., 1982; Fessel and Snedeker, 2011; Chen et al., 2015). Furthermore, many multi-scale homogenization approaches have been developed to account for nanoscale effects, which are related to intermolecular cross-links and collagen mechanics (Stylianopoulos and Barocas, 2007; Tang et al., 2009; Nierenberger et al., 2013; Marino and Vairo, 2014).

4.3 Comparison between models of fluid and solid-like matrix

Lanir's model accounts for fiber volume fraction (Φ_i), the orientation ($\mathcal{R}_i$) and undulation distributions (e_0), while Holzapfel's model involves only fiber orientation (I_i). Lanir's model therefore provides high predictive power. This model, however, is not easy to implement with FE simulation due to complex integral expressions of SEF. A structural model with straightforward SEF (e.g., Holzapfel et al.'s model) may be more efficient for FE simulations. Such SEFs have been employed in FE analysis for diseased coronary arteries (Holzapfel et al., 2005a; Cardoso et al., 2014). It noted that the two-layer models (accounts for individual layered microstructure) are typically used as the intima contributes negligible mechanical support for coronary arteries of normal animals, normal animals. For those arteries with three distinct layers, however, such as coronary arteries of aged humans or animals, a three-layer microstructural model should be developed to reflect intimal responses. For instance, Holzapfel et al. (Holzapfel et al., 2005a) developed a three-layer model of normal human coronary arteries, and their analysis showed the intima has significant load-bearing capacity and mechanical strength when compared with the media and adventitia. For atherosclerotic vessels, additional layers or components should be added in the mechanical artery models (i.e., Eqs. 1) or (3)) with specific material and structural properties of each component. Although quantitative microstructural data of aged and atherosclerotic coronary arteries are limited, a few qualitative or semi-quantitative data exist. For instance, Römer et al. (Römer et al., 1998) obtained different contents of cholesterol, calcium and delipidized arterial tissue in coronary arteries with progression of atherosclerosis, and Huang et al. (Huang et al., 2001) provided different material properties of fibrous plaque, arterial wall, lipid and calcium, respectively.

Various constitutive models can be applied to coronary arteries by incorporating specific microstructural features. To simplify the process, some algorithms have been developed to automatically quantify native tissue microstructural parameters based on optical images. Image analysis technique by using the Fourier transform has been widely developed to evaluate orientation in fibrous tissues (Pourdeyhimi et al., 1997), while fiber diameter was measured by direct tracking method (Ziabari et al., 2009). More recent studies introduced automated image-based analysis tool to characterize tissue fiber network topology and describe multiple parameters of elastin and collagen microarchitecture, including fiber orientation angle, diameter, tortuosity, etc. (D'Amore et al., 2010; Koch et al., 2014). Luo et al. proposed an efficient segmentation algorithm to render and extract 3D structure of medial SMCs (Luo et al., 2015). Moreover, these structural parameters are measured based on microscopic images, which are considered to be small enough as a representative volume element with a micro-scale resolution. The parameters are typically averaged over measurements at different positions of vessel walls and hence are statistically average values representative of microstructure of vascular tissue. With the aid of these approaches, microstructural data of blood vessels can be extracted from optical images and integrated into mechanical models that lead to an in-depth understanding of vessel responses.

5 FINITE ELEMENT ANALYSES OF ATHEROSCLEROSIS CORONARY ARTERIES

FE approaches are employed for diseased arteries due to the irregular shapes of fatty plaques and complex nonlinear arterial boundary conditions. FE analysis of atherosclerotic arteries is of great interest in basic and applied research as it can simulate interactions between arterial walls and stents and extensively explore tissue responses to device implantation (Chen et al., 2009; Chen et al., 2015, 2013, 2011).

In computational simulations, the behavior of plaque tissue is generally considered to be hyperplastic and with a regular shape, such as sphere, ellipse, core, etc (Chau et al., 2004; Karimi et al., 2013). The most widely used constitutive models are homogenous models due to their relatively simple SEF (Chau et al., 2004; Conway et al., 2012; García et al., 2012; Cardoso et al., 2014). The study of Imoto et al. (Imoto et al., 2005) examined the longitudinal structural determinants of plaque vulnerability by linear elastic orthotropic models, and revealed that most common rupture point is that the shoulder of the fibrous cap. Kamalanand and Srinivasan (Kamalanand and Srinivasan, 2011) recently employed a three-dimensional Neo-Hookean model to analyze mechanical behaviors of normal and atherosclerotic vessel with 50% and 90% plaque deposition. Although homogenous models have low computational costs, structured-based constitutive models can address the natural heterogeneity of biological tissues (Chau et al., 2004). There are relatively small numbers of studies that account for plaque substructure in the constitutive models. Chau et al. (Chau et al., 2004) analyzed the stress distribution of an atherosclerotic coronary using a two-dimensional rubberlike isotropic Mooney-Rivlin model based on optical coherence tomography (OCT) images. They set different material parameters for arterial wall, fibrous plaque, lipid and calcium and found that the overall stress distribution did not change drastically in regions of interest in spite of the significant changes in model geometry. The work of Holzapfel et al. (Holzapfel et al., 2005b) employed a microstructural model (Holzapfel et al., 2005a) developed for tissue components which capture anisotropic, nonlinear and dissipative characteristics, and thus distinguish lipid and calcified FE simulation of coronary stent angioplasty. Mortier et al.(Mortier et al., 2010) later employed this model to assess the effects on restenosis reduction of three drug-eluting stents.

Cardoso and Weinbaum (Cardoso and Weinbaum, 2014) demenstrated that acute coronary syndrome was largely induced by the rupture of the thin fibrous cap overlying the necrotic core of a vulnerable plaque. The rupture usually occurs when the stress of a lesion goes beyond the ultimate stress (i.e., peak circumferential stress at failure). Therefore, an accurate prediction of local stress distribution is essential for assessment of vulnerable plaque stability. A recent study (Cardoso et al., 2014) evaluated the effects of tissue material properties and geometries on the stability of vulnerable cap by three different hyperelastic constitutive models: Neo-Hookean, Mooney-Rivlin model and Holzapfel's model (Holzapfel et al., 2000). They pointed out that stress concentration factor depends on tissue properties, anisotropy, size and shape, all of which can only be accounted for by a structural mechanical model. These application and evaluations indicate microstructure-based anisotropic models can lead to a better understanding of arterial biomechanics and shed light on the very significant clinical problem of plaque rupture.

6 FUTURE PERSPECTIVES AND CHALLENGES

Microstructure-based models are a promising approach for cardiovascular biomechanics which may lead to development of computer-assisted clinical diagnosis and therapy. A very exciting application of the approach is patient-specific computational analysis based on medical imaging to provide diagnosis, virtual planning of therapy and prediction of prognosis. Realistic geometries of diseased vessels acquired by IVUS, OCT, computed tomography (CT), and magnetic resonance imaging (MRI), etc., can provide patient-specific models (Wallis de Vries et al., 2008; Holzapfel et al., 2014). IVUS allows for 3D reconstruction of *in vivo* arteries and can distinguish between tissue by using a radiofrequency spectral approach (Imoto et al., 2005; Moore et al., 1998; Nasu et al., 2006). OCT is a high resolution *in vivo* imaging modality (Chau et al., 2004; Yabushita et al., 2002), and MRI can create detailed 3D images of the arterial geometry and composition (Li et al., 2006, 2012; Sadat et al., 2010; see reviews in Wallis de Vries et al., 2008; Holzapfel et al., 2014). Moreover, the advancement of intra-arterial imaging techniques may also enable *in vivo* measurement of microstructural and molecular components (Saar et al., 2011; Yoo et al., 2011). Many studies have shown that FE analysis integrated with *in vivo* geometries provides a rational basis for investigating the biomechanical factors relevant to atherosclerosis (Chau et al., 2004; Imoto et al., 2005; Li et al., 2006; Sadat et al., 2010). Therefore, virtual assessment of device implantation prior to treatment may allow optimization of clinical outcome based on measured patient-specific geometries, microstructural arrangements, and the mechanical properties of plaques and arterial wall (i.e, SEFs). This approach requires not only accurate constitutive models but also accurate rendering of diseased arterial geometry and structure.

There is also a great need for better understanding the mechano-biological mechanisms for the disease process, which requires more detailed microstructural data of vessel wall. The smallest structures in the most current microstructural models are elastin and collagen fibril bundles and individual cells, but more data are needed on smaller structures that reflect cross-links between fiber bundles and integrin-binding between fibers and SMCs. The role of vessel tone and contraction (especially in flow regulating smaller vessels) that involves complex chemical-mechanical interaction of actin filaments in conjunction with active SMCs requires a multi-scale and multi-field homogenization models. These models, which would account for interactions between cellular actin filaments and intra-cellular elastin and collagen fibrils, would shed much needed light on the micromechanical environment of vessel wall to reveal mechanisms for the disease process. It should be noted that a multi-scale model requires mechanical properties and geometrical parameters of smaller constituents at the nanoscale and are thus restricted in clinically-relevant applications where such *in vivo* imaging resolution does not currently exist. It is expected that clinical demands will promote the development of higher resolution noninvasive imaging techniques as well as 3D image processing algorithms.

In summary, microstructural models take into consideration a full set of microstructural geometries, the interactions between constituents and the nonlinearity of materials, leading to a better understanding of cardiovascular biomechanics. Most importantly, microstructural model-based FE analysis integrated with patient-specific geometries and structure should advance computer-assisted clinical diagnosis and intervention in the future.

Acknowledgments

This work was supported by the National Institute of Health National Heart, Lung, and Blood Institute Grant 1 R01 HL117990.

REFERENCES

Adiguzel E, Ahmad PJ, Franco C, Bendeck MP. Collagens in the progression and complications of atherosclerosis. Vasc Med. 2009; 14:73–89. [PubMed: 19144782]

Annovazzi L, Genna F. An engineering, multiscale constitutive model for fiber-forming collagen in tension. J Biomed Mater Res A. 2010; 92:254–266. [PubMed: 19180522]

Antoniadis AP, Mortier P, Kassab G, Dubini G, Foin N, Murasato Y, Giannopoulos AA, Tu S, Iwasaki K, Hikichi Y, Migliavacca F, Chiastra C, Wentzel JJ, Gijsen F, Reiber JHC, Barlis P, Serruys PW, Bhatt DL, Stankovic G, Edelman ER, Giannoglou GD, Louvard Y, Chatzizisis YS. Biomechanical Modeling to Improve Coronary Artery Bifurcation Stenting: Expert Review Document on Techniques and Clinical Implementation. JACC Cardiovasc Interv. 2015; 8:1281–1296. [PubMed: 26315731]

Arribas SM, Hinek A, González MC. Elastic fibres and vascular structure in hypertension. Pharmacol. Ther. 2006; 111:771–791. [PubMed: 16488477]

Avril S, Badel P, Gabr M, Sutton MA, Lessner SM. Biomechanics of porcine renal arteries and role of axial stretch. J Biomech Eng. 2013; 135:81007. [PubMed: 23722353]

Azuma T, Hasegawa M. A rheological approach to the architecture of arterial walls. Jpn. J. Physiol. 1971; 21:27–47. [PubMed: 5317235]

Banes AJ, Baird CW, Dorofi D, Calderon M, Upchurch G, Amaya G, Keagy B, Brody A, Gauldie J. Cyclic mechanical load and growth factors stimulate endothelial and smooth muscle cell DNA synthesis. European Respiratory Review. 1993; 3:618–622.

Boulesteix T, Pena A-M, Pagès N, Godeau G, Sauviat M-P, Beaurepaire E, Schanne-Klein M-C. Micrometer scale ex vivo multiphoton imaging of unstained arterial wall structure. Cytometry A. 2006; 69:20–26. [PubMed: 16342114]

Briones AM, Arribas SM, Salaices M. Role of extracellular matrix in vascular remodeling of hypertension. Curr. Opin. Nephrol. Hypertens. 2010; 19:187–194. [PubMed: 20040870]

Bunce, DFM. Atlas of arterial histology. St. Louis: W.H. Green; 1974.

Burton AC. Relation of structure to function of the tissues of the wall of blood vessels. Physiol. Rev. 1954; 34:619–642. [PubMed: 13215088]

Burton AC, Yamada S. Relation between blood pressure and flow in the human forearm. J Appl Physiol. 1951; 4:329–339. [PubMed: 14938261]

Cardoso L, Kelly-Arnold A, Maldonado N, Laudier D, Weinbaum S. Effect of tissue properties, shape and orientation of microcalcifications on vulnerable cap stability using different hyperelastic constitutive models. J Biomech. 2014; 47:870–877. [PubMed: 24503048]

Cardoso L, Weinbaum S. Changing views of the biomechanics of vulnerable plaque rupture: a review. Ann Biomed Eng. 2014; 42:415–431. [PubMed: 23842694]

Carlson BE, Secomb TW. A theoretical model for the myogenic response based on the length-tension characteristics of vascular smooth muscle. Microcirculation. 2005; 12:327–338. [PubMed: 16020079]

Cebova M, Kristek F. Age-dependent ultrastructural changes of coronary artery in spontaneously hypertensive rats. Gen. Physiol. Biophys. 2011; 30:364–372. [PubMed: 22131318]

Chau AH, Chan RC, Shishkov M, MacNeill B, Iftimia N, Tearney GJ, Kamm RD, Bouma BE, Kaazempur-Mofrad MR. Mechanical analysis of atherosclerotic plaques based on optical coherence tomography. Ann Biomed Eng. 2004; 32:1494–1503. [PubMed: 15636110]

Chen H, Guo X, Kassab GS. A validated 3D microstructure-based constitutive model of coronary artery adventitia. In review. 2015

Chen H, Liu Y, Slipchenko MN, Zhao X, Cheng J-X, Kassab GS. The layered structure of coronary adventitia under mechanical load. Biophys. J. 2011a; 101:2555–2562. [PubMed: 22261042]

Chen H, Liu Y, Zhao X, Lanir Y, Kassab GS. A micromechanics finite-strain constitutive model of fibrous tissue. Journal of the Mechanics and Physics of Solids. 2011b; 59:1823–1837. [PubMed: 21927506]

Chen H, Luo T, Zhao X, Lu X, Huo Y, Kassab GS. Microstructural constitutive model of active coronary media. Biomaterials. 2013a; 34:7575–7583. [PubMed: 23859656]

Chen H, Slipchenko MN, Liu Y, Zhao X, Cheng J-X, Lanir Y, Kassab GS. Biaxial deformation of collagen and elastin fibers in coronary adventitia. J. Appl. Physiol. 2013b; 115:1683–1693. [PubMed: 24092692]

Chen HY, Hermiller J, Sinha AK, Sturek M, Zhu L, Kassab GS. Effects of stent sizing on endothelial and vessel wall stress: potential mechanisms for in-stent restenosis. J. Appl. Physiol. 2009; 106:1686–1691. [PubMed: 19299567]

Chen HY, Koo B-K, Bhatt DL, Kassab GS. Impact of stent mis-sizing and mis-positioning on coronary fluid wall shear and intramural stress. J. Appl. Physiol. 2013; 115:285–292. [PubMed: 23722708]

Chen HY, Koo B-K, Kassab GS. Impact of bifurcation dual stenting on endothelial shear stress. J. Appl. Physiol. 2015; 119:627–632. [PubMed: 26183473]

Chen HY, Sinha AK, Choy JS, Zheng H, Sturek M, Bigelow B, Bhatt DL, Kassab GS. Mis-sizing of stent promotes intimal hyperplasia: impact of endothelial shear and intramural stress. Am. J. Physiol. Heart Circ. Physiol. 2011; 301:H2254–H2263. [PubMed: 21926337]

Choy JS, Dang Q, Molloi S, Kassab GS. Nonuniformity of axial and circumferential remodeling of large coronary veins in response to ligation. Am. J. Physiol. Heart Circ. Physiol. 2006; 290:H1558–H1565. [PubMed: 16299258]

Choy JS, Kassab GS. Wall thickness of coronary vessels varies transmurally in the LV but not the RV: implications for local stress distribution. Am. J. Physiol. Heart Circ. Physiol. 2009; 297:H750–H758. [PubMed: 19482964]

Clark JM, Glagov S. Transmural organization of the arterial media. The lamellar unit revisited. Arteriosclerosis. 1985; 5:19–34. [PubMed: 3966906]

Conway C, Sharif F, McGarry JP, McHugh PE. A Computational Test-Bed to Assess Coronary Stent Implantation Mechanics Using a Population-Specific Approach. Cardiovasc Eng Tech. 2012; 3:374–387.

Cox RH. Basis for the altered arterial wall mechanics in the spontaneously hypertensive rat. Hypertension. 1981; 3:485–495. [PubMed: 7309210]

D'Amore A, Stella JA, Wagner WR, Sacks MS. CHARACTERIZATION OF THE COMPLETE FIBER NETWORK TOPOLOGY OF PLANAR FIBROUS TISSUES AND SCAFFOLDS. Biomaterials. 2010; 31:5345–5354. [PubMed: 20398930]

Decraemer WF, Maes MA, Vanhuyse VJ. An elastic stress-strain relation for soft biological tissues based on a structural model. J Biomech. 1980; 13:463–468. [PubMed: 7400174]

Dingemans KP, Teeling P, Lagendijk JH, Becker AE. Extracellular matrix of the human aortic media: an ultrastructural histochemical and immunohistochemical study of the adult aortic media. Anat. Rec. 2000; 258:1–14. [PubMed: 10603443]

Dobrin PB. Mechanical behavior of vascular smooth muscle in cylindrical segments of arteries in vitro. Ann Biomed Eng. 1984; 12:497–510. [PubMed: 6534220]

Faber M, MOller-Hou G. The human aorta. V. Collagen and elastin in the normal and hypertensive aorta. Acta Pathol Microbiol Scand. 1952; 31:377–382. [PubMed: 12985344]

Fessel G, Snedeker JG. Equivalent stiffness after glycosaminoglycan depletion in tendon--an ultra-structural finite element model and corresponding experiments. J. Theor. Biol. 2011; 268:77–83. [PubMed: 20950629]

Finlay HM, McCullough L, Canham PB. Three-dimensional collagen organization of human brain arteries at different transmural pressures. J. Vasc. Res. 1995; 32:301–312. [PubMed: 7578798]

Fischer GM, Llaurado JG. Collagen and elastin content in canine arteries selected from functionally different vascular beds. Circ. Res. 1966; 19:394–399. [PubMed: 5914851]

Fischer H. Über die funktionelle Bedeutung des Spiralverlaufes der Muskulatur in der Arterienwand. Gegenbaurs Morphol Jahrbuch. 1951; 91:394–445.

Folkow B, Svanborg A. Physiology of cardiovascular aging. Physiol. Rev. 1993; 73:725–764. [PubMed: 8105498]

Fridez P, Zulliger M, Bobard F, Montorzi G, Miyazaki H, Hayashi K, Stergiopulos N. Geometrical, functional, and histomorphometric adaptation of rat carotid artery in induced hypertension. J Biomech. 2003; 36:671–680. [PubMed: 12694997]

Fujiwara T, Uehara Y. The cytoarchitecture of the medial layer in rat thoracic aorta: a scanning electron-microscopic study. Cell Tissue Res. 1992; 270:165–172. [PubMed: 1423519]

García A, Peña E, Martínez MA. Influence of geometrical parameters on radial force during self-expanding stent deployment. Application for a variable radial stiffness stent. J Mech Behav Biomed Mater. 2012; 10:166–175. [PubMed: 22520428]

Garcia M, Kassab GS. Right coronary artery becomes stiffer with increase in elastin and collagen in right ventricular hypertrophy. J. Appl. Physiol. 2009; 106:1338–1346. [PubMed: 19179652]

Gasser TC, Ogden RW, Holzapfel GA. Hyperelastic modelling of arterial layers with distributed collagen fibre orientations. Journal of The Royal Society Interface. 2006; 3:15–35.

Gasser TC, Schulze-Bauer CAJ, Holzapfel GA. A three-dimensional finite element model for arterial clamping. J Biomech Eng. 2002; 124:355–363. [PubMed: 12188202]

Gentleman E, Lay AN, Dickerson DA, Nauman EA, Livesay GA, Dee KC. Mechanical characterization of collagen fibers and scaffolds for tissue engineering. Biomaterials. 2003; 24:3805–3813. [PubMed: 12818553]

Glagov S, Vito R, Giddens DP, Zarins CK. Micro-architecture and composition of artery walls: relationship to location, diameter and the distribution of mechanical stress. J Hypertens. 1992; (Suppl 10):S101–S104.

Gosline J, Lillie M, Carrington E, Guerette P, Ortlepp C, Savage K. Elastic proteins: biological roles and mechanical properties. Philos Trans R Soc Lond B Biol Sci. 2002; 357:121–132. [PubMed: 11911769]

Greenwald S. Ageing of the conduit arteries. J. Pathol. 2007; 211:157–172. [PubMed: 17200940]

Grytz R, Meschke G. Constitutive modeling of crimped collagen fibrils in soft tissues. J Mech Behav Biomed Mater. 2009; 2:522–533. [PubMed: 19627859]

Gundiah N, B Ratcliffe M, A Pruitt L. Determination of strain energy function for arterial elastin: Experiments using histology and mechanical tests. J Biomech. 2007; 40:586–594. [PubMed: 16643925]

Haas KS, Phillips SJ, Comerota AJ, White JV. The architecture of adventitial elastin in the canine infrarenal aorta. Anat. Rec. 1991; 230:86–96. [PubMed: 2064031]

Hansen TR, Dineen DX, Pullen GL. Orientation of arterial smooth muscle and strength of contraction of aortic strips from DOCA-hypertensive rats. Blood Vessels. 1980; 17:302–311. [PubMed: 7437523]

Hass GM. Elastic tissue. II. A study of the elasticity and tensile strength of elastic tissue isolated from the human aorta. Arch. Path. 1942; 34:971.

Hayman DM, Zhang J, Liu Q, Xiao Y, Han H-C. Smooth muscle cell contraction increases the critical buckling pressure of arteries. J Biomech. 2013; 46:841–844. [PubMed: 23261241]

Hollander Y, Durban D, Lu X, Kassab GS, Lanir Y. Experimentally Validated Micro Structural 3D Constitutive Model of Coronary Arterial Media. J Biomech Eng. 2011; 133:031007. [PubMed: 21303183]

Holzapfel GA, Gasser TC, Ogden RW. A New Constitutive Framework for Arterial Wall Mechanics and a Comparative Study of Material Models. Journal of Elasticity. 2000; 61:1–48.

Holzapfel GA, Mulvihill JJ, Cunnane EM, Walsh MT. Computational approaches for analyzing the mechanics of atherosclerotic plaques: a review. J Biomech. 2014; 47:859–869. [PubMed: 24491496]

Holzapfel GA, Sommer G, Gasser CT, Regitnig P. Determination of layer-specific mechanical properties of human coronary arteries with nonatherosclerotic intimal thickening and related constitutive modeling. Am. J. Physiol. Heart Circ. Physiol. 2005a; 289:H2048–H2058. [PubMed: 16006541]

Holzapfel GA, Stadler M, Gasser TC. Changes in the mechanical environment of stenotic arteries during interaction with stents: computational assessment of parametric stent designs. J Biomech Eng. 2005b; 127:166–180. [PubMed: 15868799]

Huang H, Virmani R, Younis H, Burke AP, Kamm RD, Lee RT. The impact of calcification on the biomechanical stability of atherosclerotic plaques. Circulation. 2001; 103:1051–1056. [PubMed: 11222465]

Humphrey JD, Yin FC. A new constitutive formulation for characterizing the mechanical behavior of soft tissues. Biophys J. 1987; 52:563–570. [PubMed: 3676437]

Huo Y, Cheng Y, Zhao X, Lu X, Kassab GS. Biaxial vasoactivity of porcine coronary artery. Am. J. Physiol. Heart Circ. Physiol. 2012; 302:H2058–H2063. [PubMed: 22427520]

Huo Y, Zhao X, Cheng Y, Lu X, Kassab GS. Two-layer model of coronary artery vasoactivity. J. Appl. Physiol. 2013; 114:1451–1459. [PubMed: 23471951]

Imoto K, Hiro T, Fujii T, Murashige A, Fukumoto Y, Hashimoto G, Okamura T, Yamada J, Mori K, Matsuzaki M. Longitudinal structural determinants of atherosclerotic plaque vulnerability: a computational analysis of stress distribution using vessel models and three-dimensional intravascular ultrasound imaging. J. Am. Coll. Cardiol. 2005; 46:1507–1515. [PubMed: 16226176]

Kamalanand K, Srinivasan S. Modelling and analysis of normal and atherosclerotic blood vessel mechanics using 3D finite element models. ICTACT Journal on Soft Computing. 2011; 2:261–264.

Karimi A, Navidbakhsh M, Shojaei A, Faghihi S. Measurement of the uniaxial mechanical properties of healthy and atherosclerotic human coronary arteries. Mater Sci Eng C Mater Biol Appl. 2013; 33:2550–2554. [PubMed: 23623067]

Klein L, Gheorghiade M. Coronary artery disease and prevention of heart failure. Med. Clin. North Am. 2004; 88:1209–1235. [PubMed: 15331314]

Kochová P, Kuncová J, Svíglerová J, Cimrman R, Miklíková M, Liška V, Tonar Z. The contribution of vascular smooth muscle, elastin and collagen on the passive mechanics of porcine carotid arteries. Physiol Meas. 2012; 33:1335–1351. [PubMed: 22813960]

Koch RG, Tsamis A, D'Amore A, Wagner WR, Watkins SC, Gleason TG, Vorp DA. A custom image-based analysis tool for quantifying elastin and collagen micro-architecture in the wall of the human aorta from multi-photon microscopy. J Biomech. 2014; 47:935–943. [PubMed: 24524988]

Kroon M, Holzapfel GA. A new constitutive model for multi-layered collagenous tissues. J Biomech. 2008; 41:2766–2771. [PubMed: 18657813]

Lacolley P, Regnault V, Nicoletti A, Li Z, Michel J-B. The vascular smooth muscle cell in arterial pathology: a cell that can take on multiple roles. Cardiovasc. Res. 2012; 95:194–204. [PubMed: 22467316]

Lakatta EG. Cardiovascular aging in health. Clin. Geriatr. Med. 2000; 16:419–444. [PubMed: 10918640]

Lakatta EG. Cardiovascular regulatory mechanisms in advanced age. Physiological Reviews. 1993; 73:413–467. [PubMed: 8475195]

Lanir Y. Constitutive equations for fibrous connective tissues. J Biomech. 1983; 16:1–12. [PubMed: 6833305]

Lanir Y. A structural theory for the homogeneous biaxial stress-strain relationships in flat collagenous tissue. J Biomech. 1979; 12:423–436. [PubMed: 457696]

Leung DY, Glagov S, Mathews MB. Cyclic stretching stimulates synthesis of matrix components by arterial smooth muscle cells in vitro. Science. 1976; 191:475–477. [PubMed: 128820]

Li D, Robertson AM. A structural multi-mechanism constitutive equation for cerebral arterial tissue. International Journal of Solids and Structures. 2009; 46:2920–2928.

Li T, Li X, Zhao X, Zhou W, Cai Z, Yang L, Guo A, Zhao S. Classification of human coronary atherosclerotic plaques using ex vivo high-resolution multicontrast-weighted MRI compared with histopathology. AJR Am J Roentgenol. 2012; 198:1069–1075. [PubMed: 22528895]

Li Z-Y, Howarth S, Trivedi RA, U-King-Im JM, Graves MJ, Brown A, Wang L, Gillard JH. Stress analysis of carotid plaque rupture based on in vivo high resolution MRI. Journal of Biomechanics. 2006; 39:2611–2622. [PubMed: 16256124]

Lokshin O, Lanir Y. Micro and macro rheology of planar tissues. Biomaterials. 2009; 30:3118–3127. [PubMed: 19324407]

Luo T, Chen H, Kassab GS. 3D Reconstruction of Coronary Artery Vascular Smooth Muscle Cells. Accepted. 2015

Lu P, Takai K, Weaver VM, Werb Z. Extracellular Matrix Degradation and Remodeling in Development and Disease. Cold Spring Harb Perspect Biol. 2011; 3

Lu X, Kassab GS. Vasoactivity of blood vessels using a novel isovolumic myograph. Ann Biomed Eng. 2007; 35:356–366. [PubMed: 17221307]

Lu X, Pandit A, Kassab GS. Biaxial incremental homeostatic elastic moduli of coronary artery: two-layer model. Am. J. Physiol. Heart Circ. Physiol. 2004; 287:H1663–H1669. [PubMed: 15371266]

Marino M, Vairo G. Stress and strain localization in stretched collagenous tissues via a multiscale modelling approach. Comput Methods Biomech Biomed Engin. 2014; 17:11–30. [PubMed: 22525051]

Martufi G, Gasser TC. A constitutive model for vascular tissue that integrates fibril, fiber and continuum levels with application to the isotropic and passive properties of the infrarenal aorta. J Biomech. 2011; 44:2544–2550. [PubMed: 21862020]

Moiseeva EP. Adhesion receptors of vascular smooth muscle cells and their functions. Cardiovasc. Res. 2001; 52:372–386. [PubMed: 11738054]

Moore M, Spencer T, Salter D, Kearney P, Shaw T, Starkey I, Fitzgerald P, Erbel R, Lange A, McDicken N, Sutherland G, Fox K. Characterisation of coronary atherosclerotic morphology by spectral analysis of radiofrequency signal: in vitro intravascular ultrasound study with histological and radiological validation. Heart. 1998; 79:459–467. [PubMed: 9659192]

Mortier P, Holzapfel GA, De Beule M, Van Loo D, Taeymans Y, Segers P, Verdonck P, Verhegghe B. A novel simulation strategy for stent insertion and deployment in curved coronary bifurcations: comparison of three drug-eluting stents. Ann Biomed Eng. 2010; 38:88–99. [PubMed: 19898936]

Myers VC, Lang WW. Some Chemical Changes in the Human Thoracic Aorta Accompanying the Aging Process. J Gerontol. 1946; 1:441–444. [PubMed: 20273846]

Nasu K, Tsuchikane E, Katoh O, Vince DG, Virmani R, Surmely J-F, Murata A, Takeda Y, Ito T, Ehara M, Matsubara T, Terashima M, Suzuki T. Accuracy of in vivo coronary plaque morphology assessment: a validation study of in vivo virtual histology compared with in vitro histopathology. J. Am. Coll. Cardiol. 2006; 47:2405–2412. [PubMed: 16781367]

Nierenberger M, Rémond Y, Ahzi S. A new multiscale model for the mechanical behavior of vein walls. Journal of the Mechanical Behavior of Biomedical Materials. 2013; 23:32–43. [PubMed: 23660303]

Niland S, Eble JA. Integrin-Mediated Cell-Matrix Interaction in Physiological and Pathological Blood Vessel Formation. J Oncol. 2012

O'Connell MK, Murthy S, Phan S, Xu C, Buchanan J, Spilker R, Dalman RL, Zarins CK, Denk W, Taylor CA. The three-dimensional micro- and nanostructure of the aortic medial lamellar unit measured using 3D confocal and electron microscopy imaging. Matrix Biol. 2008; 27:171–181. [PubMed: 18248974]

Osborne-Pellegrin MJ. Some ultrastructural characteristics of the renal artery and abdominal aorta in the rat. J. Anat. 1978; 125:641–652. [PubMed: 640965]

Osborne-Pellegrin M, Labat C, Mercier N, Challande P, Lacolley P. Changes in aortic stiffness related to elastic fiber network anomalies in the Brown Norway rat during maturation and aging. Am. J. Physiol. Heart Circ. Physiol. 2010; 299:H144–H152. [PubMed: 20435849]

Ozolanta I, Tetere G, Purinya B, Kasyanov V. Changes in the mechanical properties, biochemical contents and wall structure of the human coronary arteries with age and sex. Med Eng Phys. 1998; 20:523–533. [PubMed: 9832028]

Pourdeyhimi B, Dent R, Davis H. Measuring Fiber Orientation in Nonwovens Part III: Fourier Transform. Textile Research Journal. 1997; 67:143–151.

Rachev A, Hayashi K. Theoretical study of the effects of vascular smooth muscle contraction on strain and stress distributions in arteries. Ann Biomed Eng. 1999; 27:459–468. [PubMed: 10468230]

Rafieian-Kopaei M, Setorki M, Doudi M, Baradaran A, Nasri H. Atherosclerosis: process, indicators, risk factors and new hopes. Int J Prev Med. 2014; 5:927–946. [PubMed: 25489440]

Rhodin JA. Fine structure of vascular walls in mammals with special reference to smooth muscle component. Physiol Rev. 1962; (Suppl 5):48–87.

Rhodin, JAG. Handbook of Physiology, The Cardiovascular System, Vascular Smooth Muscle. Bethesda: American Physiology Society; 1980. Architecture of the Vessel Wall; p. 1-31.

Roach MR, Burton AC. The reason for the shape of the distensibility curves of arteries. Can J Biochem Physiol. 1957; 35:681–690. [PubMed: 13460788]

Robert L. Aging of the vascular wall and atherogenesis: role of the elastin-laminin receptor. Atherosclerosis. 1996; 123:169–179. [PubMed: 8782848]

Roger VL, Go AS, Lloyd-Jones DM, Benjamin EJ, Berry JD, Borden WB, Bravata DM, Dai S, Ford ES, Fox CS, Fullerton HJ, Gillespie C, Hailpern SM, Heit JA, Howard VJ, Kissela BM, Kittner SJ, Lackland DT, Lichtman JH, Lisabeth LD, Makuc DM, Marcus GM, Marelli A, Matchar DB, Moy CS, Mozaffarian D, Mussolino ME, Nichol G, Paynter NP, Soliman EZ, Sorlie PD, Sotoodehnia N, Turan TN, Virani SS, Wong ND, Woo D, Turner MB. Heart Disease and Stroke Statistics—2012 Update A Report From the American Heart Association. Circulation. 2012; 125:e2–e220. [PubMed: 22179539]

Römer TJ, Brennan JF, Fitzmaurice M, Feldstein ML, Deinum G, Myles JL, Kramer JR, Lees RS, Feld MS. Histopathology of human coronary atherosclerosis by quantifying its chemical composition with Raman spectroscopy. Circulation. 1998; 97:878–885. [PubMed: 9521336]

Saar BG, Johnston RS, Freudiger CW, Xie XS, Seibel EJ. Coherent Raman scanning fiber endoscopy. Opt Lett. 2011; 36:2396–2398. [PubMed: 21725423]

Sadat U, Li Z-Y, Young VE, Graves MJ, Boyle JR, Warburton EA, Varty K, O'Brien E, Gillard JH. Finite element analysis of vulnerable atherosclerotic plaques: a comparison of mechanical stresses within carotid plaques of acute and recently symptomatic patients with carotid artery disease. J Neurol Neurosurg Psychiatry. 2010; 81:286–289. [PubMed: 19939857]

Sáez P, Peña E, Martínez MA. A structural approach including the behavior of collagen cross-links to model patient-specific human carotid arteries. Ann Biomed Eng. 2014; 42:1158–1169. [PubMed: 24639211]

Schlatmann TJ, Becker AE. Histologic changes in the normal aging aorta: implications for dissecting aortic aneurysm. Am. J. Cardiol. 1977; 39:13–20. [PubMed: 831420]

Schwartz CJ, Valente AJ, Sprague EA, Kelley JL, Nerem RM. The pathogenesis of atherosclerosis: an overview. Clin Cardiol. 1991; 14:I1–I16. [PubMed: 2044253]

Shadwick RE. Mechanical design in arteries. J. Exp. Biol. 1999; 202:3305–3313. [PubMed: 10562513]

Silver FH, Snowhill PB, Foran DJ. Mechanical Behavior of Vessel Wall: A Comparative Study of Aorta, Vena Cava, and Carotid Artery. Annals of Biomedical Engineering. 2003; 31:793–803. [PubMed: 12971612]

Smith JF, Canham PB, Starkey J. Orientation of collagen in the tunica adventitia of the human cerebral artery measured with polarized light and the universal stage. J. Ultrastruct. Res. 1981; 77:133–145. [PubMed: 6171651]

Sokolis DP, Kefaloyannis EM, Kouloukoussa M, Marinos E, Boudoulas H, Karayannacos PE. A structural basis for the aortic stress-strain relation in uniaxial tension. J Biomech. 2006; 39:1651–1662. [PubMed: 16045914]

Stary HC, Chandler AB, Dinsmore RE, Fuster V, Glagov S, Insull W, Rosenfeld ME, Schwartz CJ, Wagner WD, Wissler RW. A Definition of Advanced Types of Atherosclerotic Lesions and a Histological Classification of Atherosclerosis A Report From the Committee on Vascular Lesions of the Council on Arteriosclerosis, American Heart Association. Circulation. 1995; 92:1355–1374. [PubMed: 7648691]

Stout LC, Whorton EB, Vaghela M. Pathogenesis of diffuse intimal thickening (DIT) in non-human primate thoracic aortas. Atherosclerosis. 1983; 47:1–6. [PubMed: 6870983]

Stylianopoulos T, Barocas VH. Multiscale, structure-based modeling for the elastic mechanical behavior of arterial walls. J Biomech Eng. 2007; 129:611–618. [PubMed: 17655483]

Tang H, Buehler MJ, Moran B. A constitutive model of soft tissue: from nanoscale collagen to tissue continuum. Ann Biomed Eng. 2009; 37:1117–1130. [PubMed: 19353270]

Thubrikar MJ, Robicsek F. Pressure-induced arterial wall stress and atherosclerosis. Ann. Thorac. Surg. 1995; 59:1594–1603. [PubMed: 7771858]

Toda T, Tsuda N, Nishimori I, Leszczynski DE, Kummerow FA. Morphometrical analysis of the aging process in human arteries and aorta. Acta Anat (Basel). 1980; 106:35–44. [PubMed: 7415788]

Tsamis A, Krawiec JT, Vorp DA. Elastin and collagen fibre microstructure of the human aorta in ageing and disease: a review. J R Soc Interface. 2013; 10:20121004. [PubMed: 23536538]

Valenta J, Svoboda J, Valerianova D, Vitek K. Residual strain in human atherosclerotic coronary arteries and age related geometrical changes. Biomed Mater Eng. 1999; 9:311–317. [PubMed: 10822486]

Valenta J, Vitek K, Cihak R, Konvickova S, Sochor M, Horny L. Age related constitutive laws and stress distribution in human main coronary arteries with reference to residual strain. Biomed Mater Eng. 2002; 12:121–134. [PubMed: 12122236]

Velican C, Velican D. Study of coronary intimal thickening. Atherosclerosis. 1985; 56:331–344. [PubMed: 4052151]

Velican D, Velican C. Accelerated atherosclerosis in subjects with some minor deviations from the common type of distribution of human coronary arteries. Atherosclerosis. 1981a; 40:309–320. [PubMed: 7332610]

Velican D, Velican C. Comparative study on age-related changes and atherosclerotic involvement of the coronary arteries of male and female subjects up to 40 years of age. Atherosclerosis. 1981b; 38:39–50. [PubMed: 7470204]

Viidik, A. Biomechanical behavior of soft connective tissues, in. In: Akkas, N., editor. Progress in Biomechanics. 1979. p. 75-113.

Viidik A, Danielson CC, Oxlund H. On fundamental and phenomenological models, structure and mechanical properties of collagen, elastin and glycosaminoglycan complexes. Biorheology. 1982; 19:437–451. [PubMed: 6286009]

Virmani R, Avolio AP, Mergner WJ, Robinowitz M, Herderick EE, Cornhill JF, Guo SY, Liu TH, Ou DY, O'Rourke M. Effect of aging on aortic morphology in populations with high and low prevalence of hypertension and atherosclerosis. Comparison between occidental and Chinese communities. Am. J. Pathol. 1991; 139:1119–1129. [PubMed: 1951629]

Virmani R, Kolodgie FD, Burke AP, Farb A, Schwartz SM. Lessons From Sudden Coronary Death A Comprehensive Morphological Classification Scheme for Atherosclerotic Lesions. Arterioscler Thromb Vasc Biol. 2000; 20:1262–1275. [PubMed: 10807742]

Walker-Caprioglio HM, Trotter JA, Mercure J, Little SA, McGuffee LJ. Organization of rat mesenteric artery after removal of cells or extracellular matrix components. Cell Tissue Res. 1991; 264:63–77. [PubMed: 2054846]

Wallis de Vries BM, van Dam GM, Tio RA, Hillebrands J-L, Slart RHJA, Zeebregts CJ. Current imaging modalities to visualize vulnerability within the atherosclerotic carotid plaque. Journal of Vascular Surgery. 2008; 48:1620–1629. [PubMed: 18804942]

Wang C, Garcia M, Lu X, Lanir Y, Kassab GS. Three-dimensional mechanical properties of porcine coronary arteries: a validated two-layer model. Am. J. Physiol. Heart Circ. Physiol. 2006; 291:H1200–H1209. [PubMed: 16582016]

Wan W, Dixon JB, Gleason RL. Constitutive modeling of mouse carotid arteries using experimentally measured microstructural parameters. Biophys. J. 2012; 102:2916–2925. [PubMed: 22735542]

Ward MR, Pasterkamp G, Yeung AC, Borst C. Arterial Remodeling Mechanisms and Clinical Implications. Circulation. 2000; 102:1186–1191. [PubMed: 10973850]

Wei JY. Age and the Cardiovascular System. New England Journal of Medicine. 1992; 327:1735–1739. [PubMed: 1304738]

Wolinsky H, Glagov S. A lamellar unit of aortic medial structure and function in mammals. Circ. Res. 1967; 20:99–111. [PubMed: 4959753]

Wuyts FL, Vanhuyse VJ, Langewouters GJ, Decraemer WF, Raman ER, Buyle S. Elastic properties of human aortas in relation to age and atherosclerosis: a structural model. Phys Med Biol. 1995; 40:1577–1597. [PubMed: 8532741]

Yabushita H, Bouma BE, Houser SL, Aretz HT, Jang I-K, Schlendorf KH, Kauffman CR, Shishkov M, Kang D-H, Halpern EF, Tearney GJ. Characterization of Human Atherosclerosis by Optical Coherence Tomography. Circulation. 2002; 106:1640–1645. [PubMed: 12270856]

Yoo H, Kim JW, Shishkov M, Namati E, Morse T, Shubochkin R, McCarthy JR, Ntziachristos V, Bouma BE, Jaffer FA, Tearney GJ. Intra-arterial catheter for simultaneous microstructural and molecular imaging in vivo. Nat Med. 2011; 17:1680–1684. [PubMed: 22057345]

Zhang W, Herrera C, Atluri SN, Kassab GS. Effect of surrounding tissue on vessel fluid and solid mechanics. J Biomech Eng. 2004; 126:760–769. [PubMed: 15796334]

Ziabari M, Mottaghitalab V, Haghi AK. Application of direct tracking method for measuring electrospun nanofiber diameter. Brazilian Journal of Chemical Engineering. 2009; 26:53–62.

Zoumi A, Lu X, Kassab GS, Tromberg BJ. Imaging coronary artery microstructure using second-harmonic and two-photon fluorescence microscopy. Biophys. J. 2004; 87:2778–2786. [PubMed: 15454469]

Zulliger MA, Fridez P, Hayashi K, Stergiopulos N. A strain energy function for arteries accounting for wall composition and structure. J Biomech. 2004a; 37:989–1000. [PubMed: 15165869]

Zulliger MA, Rachev A, Stergiopulos N. A constitutive formulation of arterial mechanics including vascular smooth muscle tone. Am. J. Physiol. Heart Circ. Physiol. 2004b; 287:H1335–H1343. [PubMed: 15130890]

Zulliger MA, Stergiopulos N. Structural strain energy function applied to the ageing of the human aorta. J Biomech. 2007; 40:3061–3069. [PubMed: 17822709]

Zwolak RM, Adams MC, Clowes AW. Kinetics of vein graft hyperplasia: association with tangential stress. J. Vasc. Surg. 1987; 5:126–136. [PubMed: 3795379]

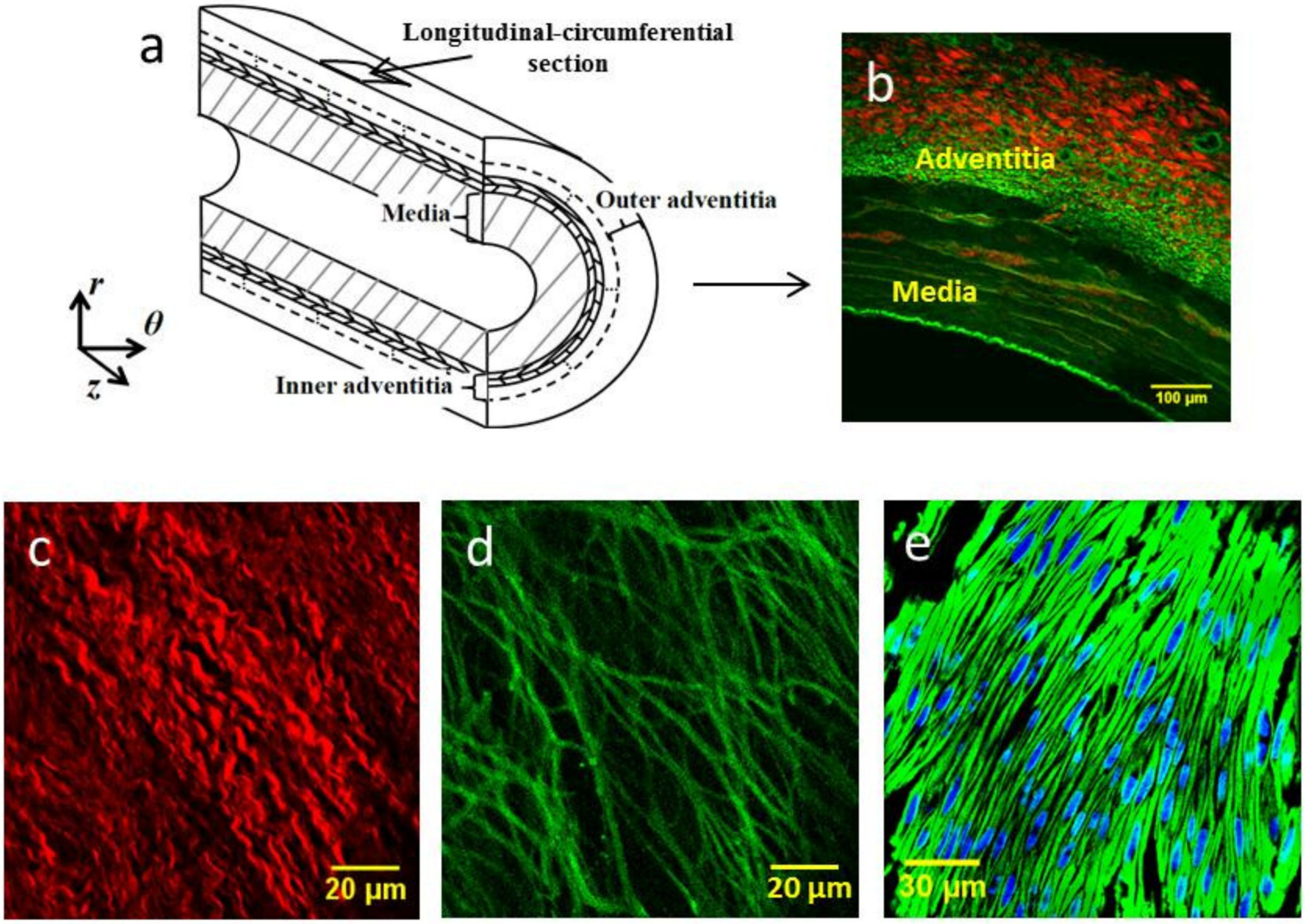

Figure 1.

(a) Schematic figure of coronary artery layered-structure (r, θ and z designate radial, circumferential and axial direction of an artery); (b): A merged SHG/TPEF image of arterial cross-section (red indicates collagen and green indicates elastin fibers); (c–d): SHG and TPEF images of longitudinal-circumferential sections of inner adventitia. (e): Confocal images of SMCs of media (F-actin was labeled by Alexa Fluor 488 Phalloidin (Green) and the cellular nucleu was labeled by DAPI (Blue)). Reproduced from (H. Chen et al., 2013a, 2011a).

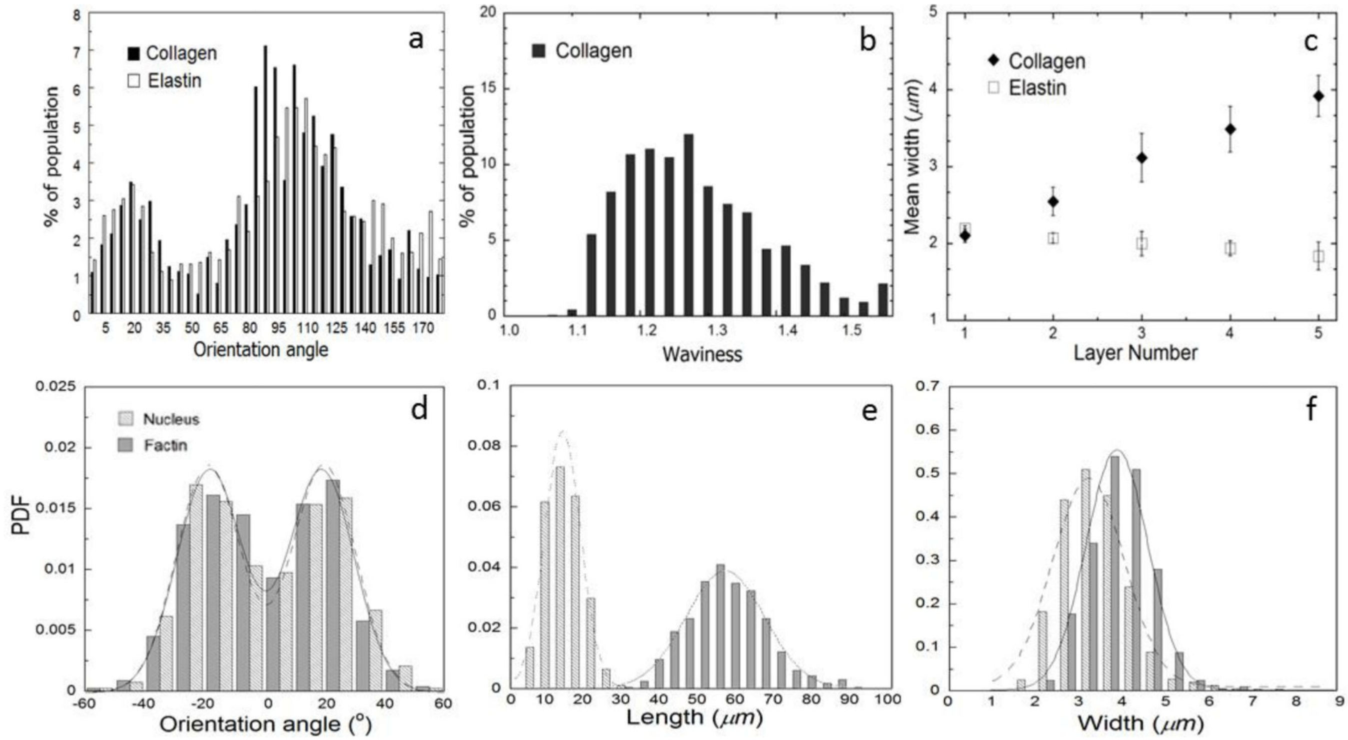

Figure 2.

Microstructural data of fibers and SMCs of coronary arteries. (a) The overall orientation distribution of collagen and elastin fibers of inner adventitia (0° and 90 ° indicate circumferential and axial directions of blood vessel, respectively); (b) The asymmetrical distribution of the collagen waviness; (c) Layer-to-layer heterogeneity of fiber width; (d) Probability density functions (PDFs) of medial SMC orientation angles; and (e–f) PDFs of SMC lengths and widths (Columns present experimental measurements and solid and dashed lines present approximated normal distributions). Reproduced from (H. Chen et al., 2013a, 2011a).

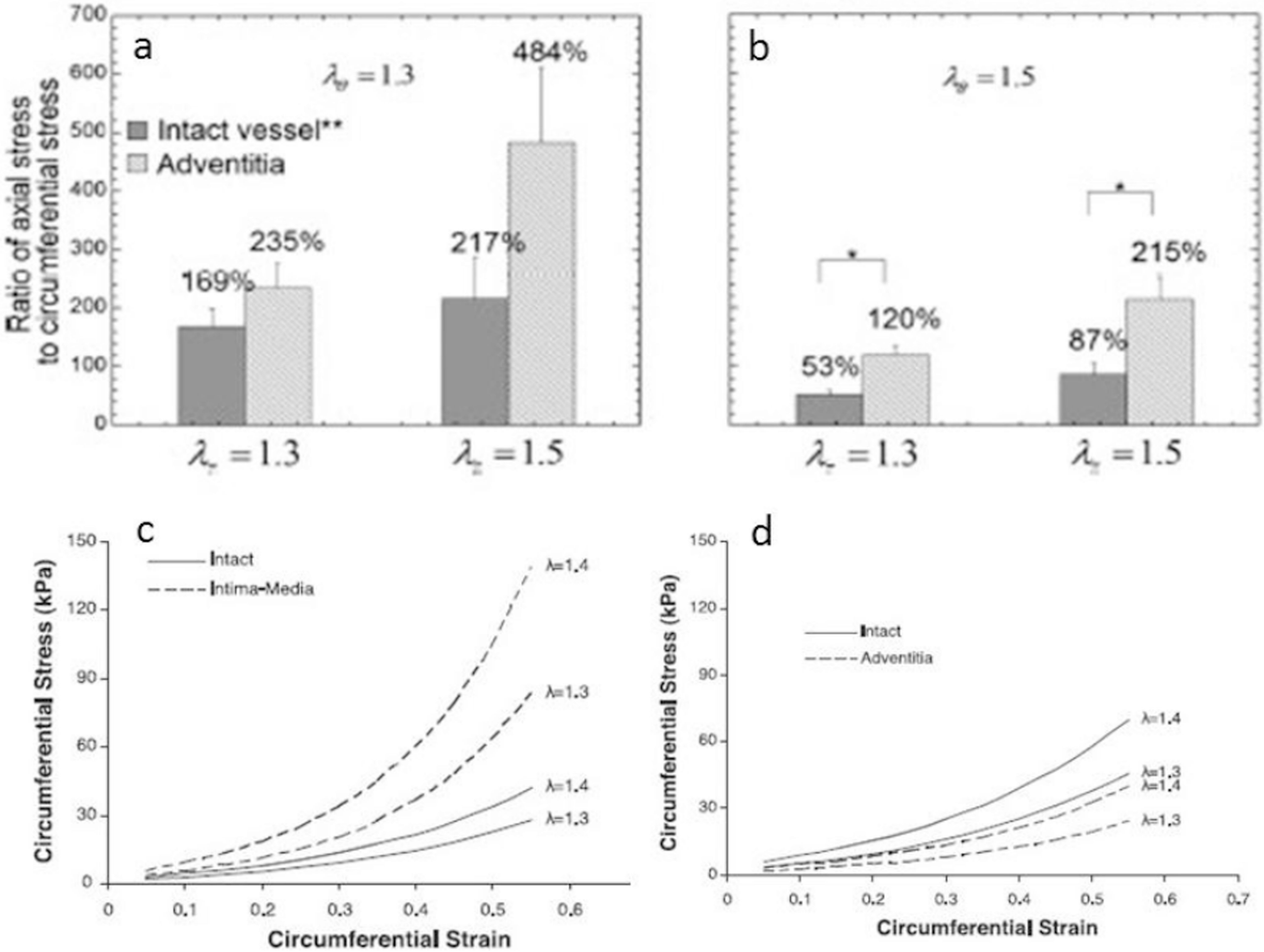

Figure 3.

Mechanical responses of individual coronary adventitia and media layers. (a–b) The ratio of axial to circumferential stress of coronary adventitia and intact vessel at different axial loads $\lambda_z = 1.3$ and $\lambda_z = 1.5 = 1.5$ with circumferential loads $\lambda_\theta = 1.3$ and $\lambda_\theta = 1.5$, respectively (*Significant differences P <0.05; Reproduced with permission from H. Chen et al., 2013b); (c–d) Stress-strain relation of adventitia, media, and intact wall of right coronary artery in circumferential direction. Data correspond to axial stretch ratios λ_z of 1.3 and 1.4. Reproduced from (Wang et al., 2006).

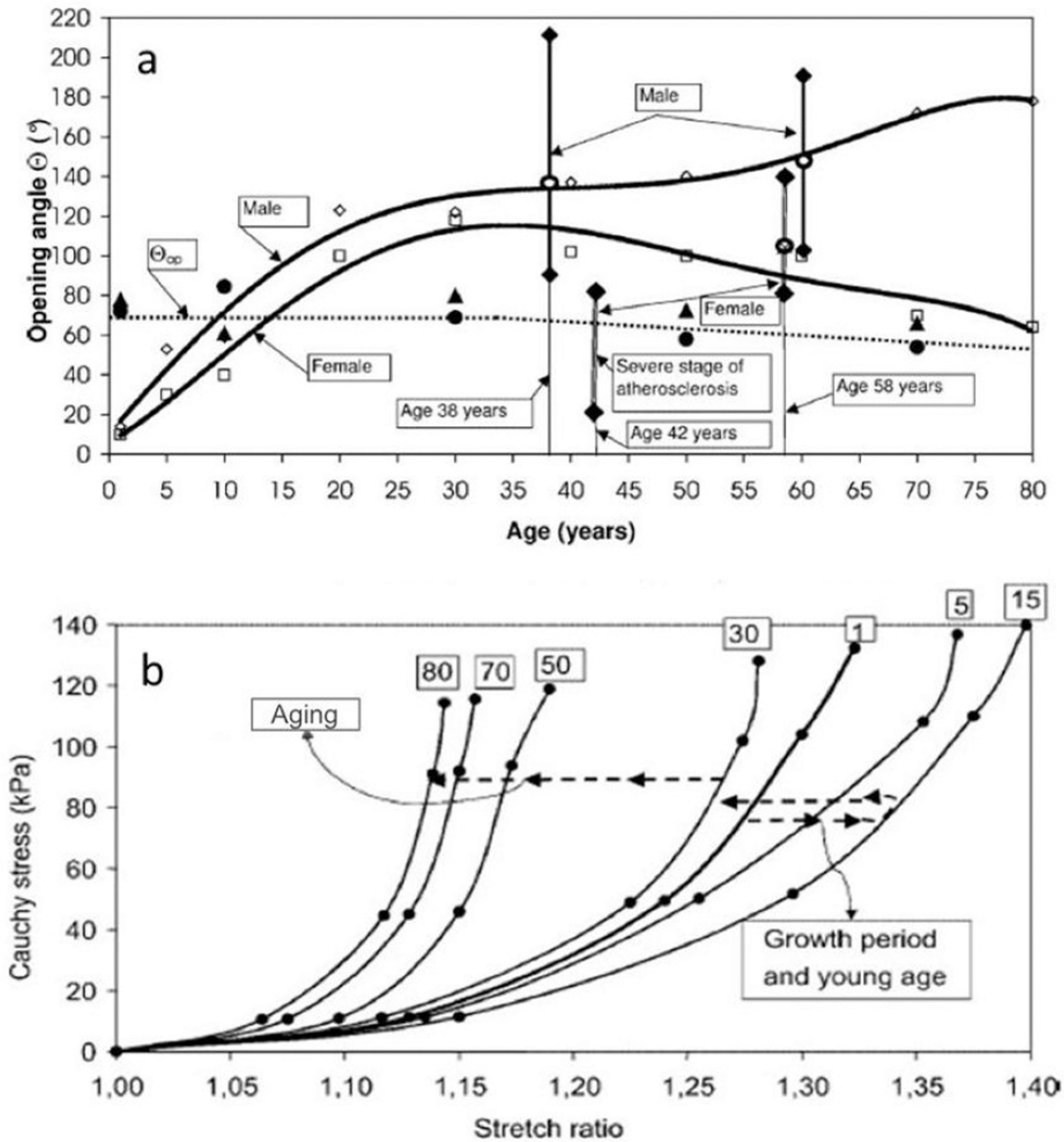

Figure 4.

Aging effects on residual strain and constitutive relation of human coronary arteries. (a) Correlation between opening angle and age; ◊ and are the average values of the predicted opening angle of the male and female coronary arteries, respectively; ♦ denotes experimental measurement of opening angles of aged human; θ_{op} is the theoretical opening angle (dotted line), corresponding to the residual strains which makes the homeostatic circumferential stress uniform in the arterial wall at normal blood pressure (● and ▲ denote female and male, respectively). (b) A constitutive relation of male left main coronary artery in the circumferential direction at different ages. Reproduced from Valenta et al., 2002.

Table 1

Quantitative data of SMC, elastin and collagen fibers in individual adventitia, media layers, and intact vessel wall of coronary arteries. (For orientation angle, 0° and 90° denote circumferential and axial directions of blood vessel, respectively).

		Adventitia	Media	Intact vessel
Opening Angle		98 *	160–210 *	126–140 *
Content	SMC		74% **	
	Elastin	22–25% *	5.3% *	16% ***
	Collagen	28–33% *	20% *	48% ***
	C/E	1.1–1.5 **	3.74 *	3.07 ***
Orientation	SMC		±18.7° *	
	Elastin	115° *	NA	
	Collagen	110° *	NA	
Dimension	SMC		4μm * (width)	
			56 μm *(Length)	
	Elastin	2 μm * (width)	NA	
	Collagen	3 μm * (width)	NA	

* Data taken from studies of porcine coronary arteries (H. Chen et al., 2011a; Garcia and Kassab, 2009; Huo et al., 2013; Lu et al., 2004);

** Data from study of rat coronary artery (Cebova and Kristek, 2011);

*** Data from study for canine coronary artery (Fischer and Llaurado, 1966).

Table 2

Changes in structural and mechanical parameters of the human left coronary arteries of with age (Sex: male). Table was assembled from data of paper (Ozolanta et al., 1998).

Age group (Years)	Wall thickness (mm)	Outer diameter (mm)	Circumferential stretch ratio	Tangential elastic modulus (MPa)	Collagen*	Elastin*
1(0–1)	0.20±0.03	1.26±0.15	1.47±0.10	1.17±0.41	40.7±1.65	7.5±0.7
2(1–7)	0.40±0.10	1.90±0.11	1.39±0.06	1.12±0.26	25.3±1.26	10.0±0.7
3(8–19)	0.43±0.12	2.28±0.18	1.39±0.05	0.90±0.48	25.0±2.59	4.88±0.8
4(20–39)	0.75±0.24	3.42±0.93	1.24±0.09	1.57±0.58	26.5±6.48	7.5±1.8
5(40–59)	0.69±0.21	3.43±1.07	1.19±0.13	2.19±0.74	27.4±3.43	9.0±2.76
6(60–80)	0.83±0.31	3.48±0.90	1.17±0.12	4.11±0.89	32.5±11.2	9.1±1.63

* Unit of fiber content is g/100g dry defatted tissue.

Author Manuscript
Author Manuscript
Author Manuscript

Table 3

Comparison of the maximum stress and strain, and physiological and maximum elastic modulus of healthy and atherosclerotic human coronary artery.).

Table was assembled from data of paper (Karimi et al., 2013).

Group	Age	Maximum stress (MPa)	Maximum strain	Physiological elastic modulus (MPa)	Maximum elastic modulus (MPa)
Healthy	38±8.6	1.44±0.87	0.54±0.25	1.48±0.24	1.55±0.26
Atherosclerosis	65.5±10.3	2.08±0.86	0.35±0.11	3.77±0.38	4.53±0.43